UNICO I+D Project
6G-INTEGRATION-4

E16-6G-INTEGRATION-4

Main flight control equations

Abstract

This deliverable contains the first development stages of the longitudinal stability and control equations of the double blimp airship as a part of the HAPS 3G-INTEGRATION -4 system. It defines the equations for both blimps and the central wing. Besides that, the characterization of some of the main terms of the equations are described, such as the engines thrust, the aerodynamic of the wings and tail fins and the aerodynamic of the whole blimp using the Jones-DeLaurier model. We are currently working on the complete development and integration of the equations to use them as a useful tool for optimization of the geometric parameters of the airship design and to feed the future auto-pilot system.

Financiado por la Unión Europea NextGenerationEU
GOBIERNO DE ESPAÑA
MINISTERIO DE ASUNTOS ECONÓMICOS Y TRANSFORMACIÓN DIGITAL
SECRETARÍA DE ESTADO DE TELECOMUNICACIONES E INFRAESTRUCTURAS DIGITALES
Plan de Recuperación, Transformación y Resiliencia

Document properties

Document number	E16-6G-INTEGRATION-4
Document title	Main flight control equations
Document responsible	Eduardo Cano Corral (Edair Technologies)
Document editor	Raul Herrero Moreno (Edair Technologies)
Editorial team	Pedro Baquero Jaén (Edair Technologies)
Target dissemination level	Public
Status of the document	Final
Version	1.0
Delivery date	30-06-2023
Actual delivery date	30-06-2023

Production properties

Reviewers	Eduardo Arca Ramirez (Edair Technologies) Daniel Segovia Vargas (UC3M)

SEGOVIA VARGAS DANIEL - 50831780D

Firmado digitalmente por SEGOVIA VARGAS DANIEL - 50831780D
Fecha: 2023.11.05 15:57:09 +01'00'

Disclaimer

This document has been produced in the context of the 6G-INTEGRATION-4 Project. The research leading to these results has received funding from the Spanish Ministry of Economic Affairs and Digital Transformation and the European Union-Next Generation EU through the UNICO 5G I+D programme.

Financiado por la Unión Europea NextGenerationEU
GOBIERNO DE ESPAÑA
MINISTERIO DE ASUNTOS ECONÓMICOS Y TRANSFORMACIÓN DIGITAL
Plan de Recuperación, Transformación y Resiliencia
UNICO I+D

Contents

Financiado por la Unión Europea NextGenerationEU
GOBIERNO DE ESPAÑA
MINISTERIO DE ASUNTOS ECONÓMICOS Y TRANSFORMACIÓN DIGITAL
SECRETARÍA DE ESTADO DE TELECOMUNICACIONES E INFRAESTRUCTURAS DIGITALES
Plan de Recuperación, Transformación y Resiliencia
UNICO I+D

Table of Figures

Financiado por la Unión Europea NextGenerationEU
GOBIERNO DE ESPAÑA
MINISTERIO DE ASUNTOS ECONÓMICOS Y TRANSFORMACIÓN DIGITAL
SECRETARÍA DE ESTADO DE TELECOMUNICACIONES E INFRAESTRUCTURAS DIGITALES
Plan de Recuperación, Transformación y Resiliencia
UNICO I+D

Table of Tables

Financiado por la Unión Europea NextGenerationEU
GOBIERNO DE ESPAÑA
MINISTERIO DE ASUNTOS ECONÓMICOS Y TRANSFORMACIÓN DIGITAL
SECRETARÍA DE ESTADO DE TELECOMUNICACIONES E INFRAESTRUCTURAS DIGITALES
Plan de Recuperación, Transformación y Resiliencia
UNICO I+D

Table of Equations

Financiado por la Unión Europea NextGenerationEU
GOBIERNO DE ESPAÑA
MINISTERIO DE ASUNTOS ECONÓMICOS Y TRANSFORMACIÓN DIGITAL
SECRETARÍA DE ESTADO DE TELECOMUNICACIONES E INFRAESTRUCTURAS DIGITALES
Plan de Recuperación, Transformación y Resiliencia
UNICO I+D

List of Acronyms

HAPS: High Altitude Platform System

Financiado por la Unión Europea NextGenerationEU
GOBIERNO DE ESPAÑA
MINISTERIO DE ASUNTOS ECONÓMICOS Y TRANSFORMACIÓN DIGITAL
SECRETARÍA DE ESTADO DE TELECOMUNICACIONES E INFRAESTRUCTURAS DIGITALES
Plan de Recuperación, Transformación y Resiliencia
UNICO I+D

Resumen Ejecutivo

El presente documento contiene las definiciones, desarrollos y proceso de obtención de las ecuaciones que definen la estabilidad y control longitudinal del HAPS propuesto en el proyecto; un doble dirigible con ala central. En el documento se describen las variables, parámetros y condiciones necesarias para que la aeronave sea estable y controlable frente a variaciones del ángulo de ataque. Se presentan los siguientes grupos de ecuaciones:

- Fuerzas Horizontales en dirigibles y ala central
- Fuerzas Verticales en dirigible y ala central
- Momentos respecto al centro de flotabilidad
- Ecuación de estabilidad longitudinal
- Caracterización aerodinámica de superficies alares
- Caracterización aerodinámica del dirigible
- Caracterización del empuje de los motores

El resto del documento está redactado en inglés, de cara a maximizar el impacto del trabajo realizado en este proyecto.

Financiado por la Unión Europea NextGenerationEU
GOBIERNO DE ESPAÑA
MINISTERIO DE ASUNTOS ECONÓMICOS Y TRANSFORMACIÓN DIGITAL
SECRETARÍA DE ESTADO DE TELECOMUNICACIONES E INFRAESTRUCTURAS DIGITALES
Plan de Recuperación, Transformación y Resiliencia
UNICO I+D

Executive Summary

This document contains the definitions, developments and process of obtaining the equations that define the stability and longitudinal control of the HAPS proposed in the project; a double airship with a central wing. The document describes the variables, parameters and conditions necessary for the aircraft to be stable and controllable against variations in the angle of attack. The following groups of equations are presented:

- Horizontal forces in blimps and central wing
- Vertical forces in blimps and central wing
- Moments about the center of buoyancy
- Longitudinal stability equation
- Aerodynamic characterization of wing surfaces
- Aerodynamic characterization of the blimps
- Engine thrust characterization

The rest of the document is written in English, in order to maximize the impact of the work carried out in this project.

Financiado por la Unión Europea NextGenerationEU
GOBIERNO DE ESPAÑA MINISTERIO DE ASUNTOS ECONÓMICOS Y TRANSFORMACIÓN DIGITAL SECRETARÍA DE ESTADO DE TELECOMUNICACIONES E INFRAESTRUCTURAS DIGITALES
Plan de Recuperación, Transformación y Resiliencia
UNICO I+D

1. Introduction

The objective of this document is to illustrate the development process of the main flight control equations of a double blimp airship with a central double wing to contain equipment pods. The equations will serve to different purposes such as acting in the design process of the airship to dimension components and its geometrical situation along the blimps, assuring the stability of the airship in different flight conditions and ultimately feed the autopilot system.

This development is currently in progress so, from now on, the document will be focused in the part of the process in an advanced stage or finished.

To resume the stability of an airship, can be said:

- Airships are very stables in its lateral axis. Because of that, this will not be a major worry for the designer.
- Airships should be carefully designed to assure longitudinal stability. This problem should have a major consideration from the designer.
- Airships are statically unstable in yaw so, this part should have a special consideration in the design using vectorial thrust to counteract the circled flight tendency.

2. Reference frames

Three right-handed, cartesian reference frames are considered in the development of equations. These are the usual reference frames used to define flight dynamic parameters, in case the special nature of the airship requires a slight modification of these frames it will be indicated properly.

- Earth frame or local horizon frame
    - Origin - arbitrary, fixed relative to the surface of the Earth
    - XH axis - positive in the direction of north
    - YH axis - positive in the direction of east
    - ZH axis - positive towards the center of the Earth

In many flight dynamics applications, the Earth frame is assumed to be inertial with a flat xH,yH-plane, though the Earth frame can also be considered a spherical coordinate system with origin at the center of the Earth.

The other two reference frames are body-fixed, with origins moving along with the aircraft, typically at the center of gravity. For an aircraft that is symmetric from right-to-left, the frames can be defined as:

- Body frame
    - Origin - airplane center of gravity

Financiado por la Unión Europea NextGenerationEU
GOBIERNO DE ESPAÑA MINISTERIO DE ASUNTOS ECONÓMICOS Y TRANSFORMACIÓN DIGITAL SECRETARÍA DE ESTADO DE TELECOMUNICACIONES E INFRAESTRUCTURAS DIGITALES
Plan de Recuperación, Transformación y Resiliencia
UNICO I+D

- xb axis - positive out the nose of the aircraft in the plane of symmetry of the aircraft
- zb axis - perpendicular to the xb axis, in the plane of symmetry of the aircraft, positive below the aircraft
- yb axis - perpendicular to the xb,zb-plane, positive determined by the right-hand rule (generally, positive out the right wing)

- Wind frame
  - Origin - airplane center of gravity
  - xw axis - positive in the direction of the velocity vector of the aircraft relative to the air
  - zw axis - perpendicular to the xw axis, in the plane of symmetry of the aircraft, positive below the aircraft
  - yw axis - perpendicular to the xw,zw-plane, positive determined by the right hand rule (generally, positive to the right)

The Earth frame is a convenient frame to express aircraft translational and rotational kinematics. The Earth frame is also useful in that, under certain assumptions, it can be approximated as inertial. Additionally, one force acting on the aircraft, weight, is fixed in the +zH direction.

The body frame is often of interest because the origin and the axes remain fixed relative to the aircraft. This means that the relative orientation of the Earth and body frames describes the aircraft attitude. Also, the direction of the force of thrust is generally fixed in the body frame, though some aircraft can vary this direction, for example by thrust vectoring.

The wind frame is a convenient frame to express the aerodynamic forces and moments acting on an aircraft. In particular, the net aerodynamic force can be divided into components along the wind frame axes, with the drag force in the −xw direction and the lift force in the −zw direction.

In our case the center of gravity as origin of the body and wind frames has been substituted by the buoyancy center. The reason of that is because the buoyancy center remains positionally constant in any flight condition so it result more appropriate to calculate moments of forces in any case.

The equations have been considered separately for both blimps and central wing, so the reference frames used are attached to these different parts, being anyway parallel to each other.

In order to illustrate the problem, an initial working image of the airship is shown below.

Neither the HTP nor the VTP will have control surfaces even though they appear in the figure.

Financiado por la Unión Europea NextGenerationEU
GOBIERNO DE ESPAÑA MINISTERIO DE ASUNTOS ECONÓMICOS Y TRANSFORMACIÓN DIGITAL SECRETARÍA DE ESTADO DE TELECOMUNICACIONES E INFRAESTRUCTURAS DIGITALES
Plan de Recuperación, Transformación y Resiliencia
UNICO I+D

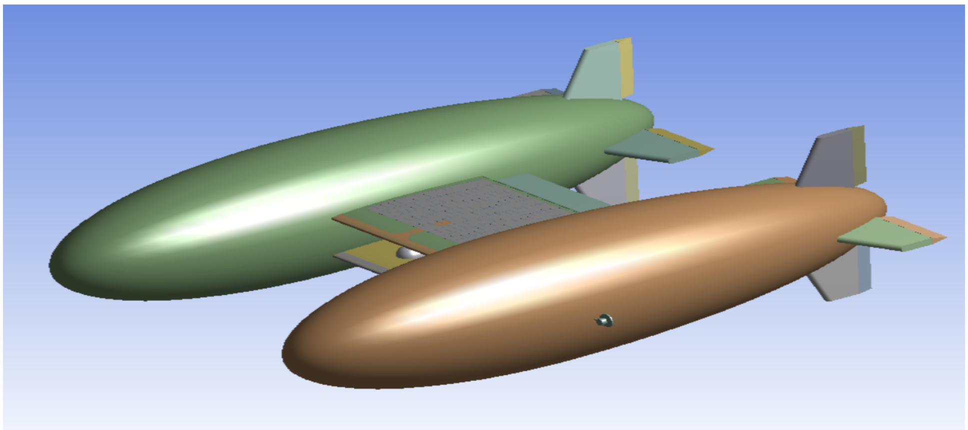

Figure 2-1 Airship working image

3. Longitudinal stability and control equations

3.1. Blimps Definitions

The longitudinal equations of stability and control for each blimp will be developed with the parameters and variables shown in the following image. Reference frames can also be seen.

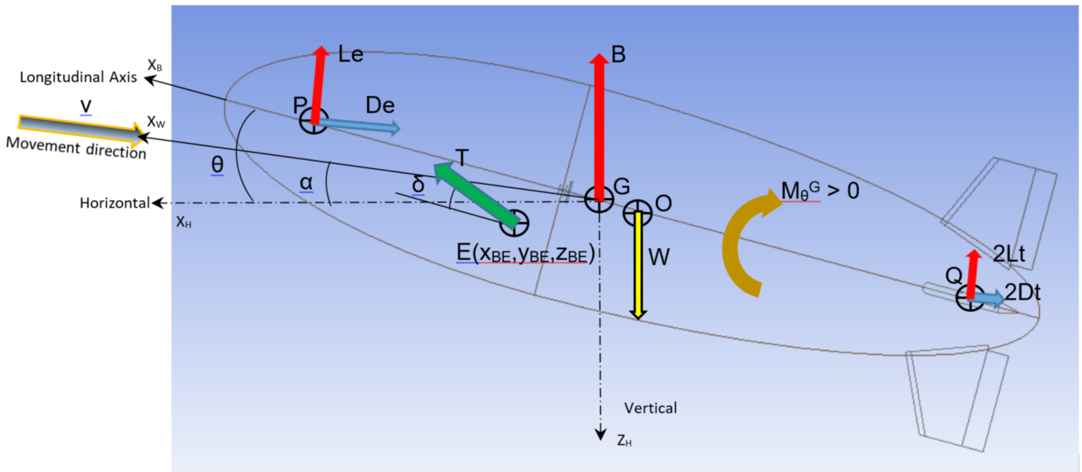

Figure 3.1-1 Longitudinal parameters and variables of a blimp

Every parameter and variable used are described below:

P · Blimp pressure center

G · Buoyancy center

Financiado por la Unión Europea NextGenerationEU
GOBIERNO DE ESPAÑA
MINISTERIO DE ASUNTOS ECONÓMICOS Y TRANSFORMACIÓN DIGITAL
SECRETARÍA DE ESTADO DE TELECOMUNICACIONES E INFRAESTRUCTURAS DIGITALES
Plan de Recuperación, Transformación y Resiliencia
UNICO I+D

O · Center of gravity

By symmetry, it is assumed that these three points are situated along X_B

Q · HTP (Horizontal Tail Plane) pressure center

It is also assumed that the projection of this point over the X_BZ_B plane is situated along X_B

E · Engine position

X_{BE},Y_{BE},Z_{BE} · Engine position coordinates in body frame

θ · Pitch angle (Angle between X_H and X_B)

α · Attack angle (Angle between X_W and X_B)

W = Blimp weight (H_2 weight not included)

ρ_a · Air density

ρ_{H2} · Hydrogen density

V · Blimp Volume

$B = \left(\rho_a - \rho_{H2}\right)Vg$ Buoyancy

v · flight velocity

$q = \frac{1}{2}\rho_a v^2$ Blimp dynamic pressure

$q_t = \frac{1}{2}\rho_a v^2 \eta_t$ HTP dynamic pressure

η_t → Tail aerodynamic efficiency

$L_e = qSC_{Le}(\alpha)$ Blimp aerodynamic lift

$D_e = qSC_{De}$ Blimp aerodynamic drag

D → Maximum diameter of the blimp

L → Maximum length of the blimp

Financiado por la Unión Europea NextGenerationEU
GOBIERNO DE ESPAÑA
MINISTERIO DE ASUNTOS ECONÓMICOS Y TRANSFORMACIÓN DIGITAL
SECRETARÍA DE ESTADO DE TELECOMUNICACIONES E INFRAESTRUCTURAS DIGITALES
Plan de Recuperación, Transformación y Resiliencia
UNICO I+D

Re → Reynolds number

$C_{De} = \frac{0.172\left(\frac{l}{D}\right)^{\frac{1}{3}} + 0.252\left(\frac{D}{l}\right)^{1.2} + 1.032\left(\frac{D}{l}\right)^{2.7}}{Re^{\frac{1}{6}}}$ Blimp aerodynamic drag coefficient (Cheeseman modelization)

$L_t = q_t S_t C_{Lt}(\alpha)$ HTP aerodynamic lift

$D_t = q_t S_t C_{Dt}(C_{Lt}, \alpha)$ HTP aerodynamic drag

$S \approx V_e^{\frac{2}{3}}$ · Blimp "wet" surface

S_t · HTP "wet" surface

T = T(power, rpm, size, propeller, etc) · Engine Thrust

Additionally, for an aerodynamic profile:

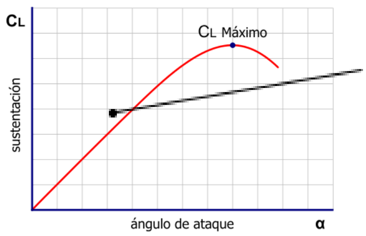

$C_L(\alpha) = a\alpha$ (depends on the chosen profile)

With all of these variables and parameters, the equations to be obtained would be:

F_H Resultant of horizontal forces in X_H axis applied in G

F_V Resultant of vertical forces in Z_H axis applied in G

M_θ^G Moment of forces respect to G

$\frac{\partial M_\theta^G}{\partial \alpha}$ Derivative of the longitudinal moment respect to α

This last equation will provide the longitudinal stability of the blimp, if this derivative value is less than zero, the airship will be stable and unstable if the value are greater than zero. This is explained because if the derivative value is less than zero implies that when the angle of attack varies in a small value due to a gust or whatever, the moment that naturally appears would be opposite to this

Financiado por la Unión Europea NextGenerationEU
GOBIERNO DE ESPAÑA MINISTERIO DE ASUNTOS ECONÓMICOS Y TRANSFORMACIÓN DIGITAL SECRETARÍA DE ESTADO DE TELECOMUNICACIONES E INFRAESTRUCTURAS DIGITALES
Plan de Recuperación, Transformación y Resiliencia
UNICO I+D

variation of α and will counteract it. Logically, if the derivative value is greater than zero, when a variation of α occurs, the moment that appears will increase the variation.

Just for clarify, the concept of stability does not imply goodness in the behavior of an airship; commercial planes and general aviation planes are designed to be stable to provide a comfortable environment for passengers or payload, however, the combat fighter planes are designed to be unstables to provide a greater agility in its maneuvers.

Logically in our case, stability is mandatory.

3.2. Blimps. Equations

Finally, with all of these definitions and considerations the equations are:

VERTICAL FORCES

$$F_V = W - B - L_e cos(\alpha) + D_e sin(\alpha) - 2L_t cos(\alpha) + 2D_t sin(\alpha) + Tsin(\theta - \delta)$$

Equation 3.2-1 **Blimps Vertical Forces**

HORIZONTAL FORCES

$$F_H = Tcos(\theta - \delta) - L_e sin(\alpha) - D_e cos(\alpha) - 2L_t sin(\alpha) - 2D_t cos(\alpha)$$

Equation 3.2-2 **Blimps Horizontal Forces**

MOMENTS RESPECT TO G

$$M_\theta^G = Tz_{BE} cos(\delta) + Tx_{BE} sin(\delta) + L_e \underline{PG} cos(\theta - \alpha) + D_e \underline{PG} sin(\theta - \alpha) - 2L_t \underline{QG} cos(\theta - \alpha) - 2D_t \underline{QG} sin(\theta - \alpha) -$$

Equation 3.2-3 **Blimps Longitudinal Moments**

DERIVATIVE RESPECT TO α OF MOMENTS (Stability Equation)

$$\frac{\partial M_\theta^G}{\partial \alpha} = \frac{\partial L_e}{\partial \alpha}\overline{PG}cos(\theta - \alpha) + L_e\overline{PG}\sin(\theta - \alpha) + \cancel{\frac{\partial D_e}{\partial \alpha}}\overline{PG}sin(\theta - \alpha) - D_e\overline{PG}\cos(\theta - \alpha) - 2\frac{\partial L_t}{\partial \alpha}\overline{QG}cos(\theta - \alpha)$$
$$- 2L_t\overline{QG}\sin(\theta - \alpha) + 2\frac{\partial D_t}{\partial \alpha}\overline{QG}sin(\theta - \alpha)$$
$$+ 2D_t\overline{QG}\cos(\theta - \alpha) + \left(4\frac{\partial D_t}{\partial \alpha}\right)z_{BE}\cos(\delta) + \left(4\frac{\partial D_t}{\partial \alpha}\right)x_{BE}\sin(\delta)$$

Equation 3.2-4 **Blimps Stability Equation**

The term crossed by an arrow is to indicate that this term is zero with the assumption that De is modeled with the Cheeseman equation (see above, page 14) which do not depends on α, so the derivative is equal to zero. However this term is included in case any other model would be used.

Financiado por la Unión Europea NextGenerationEU
GOBIERNO DE ESPAÑA
MINISTERIO DE ASUNTOS ECONÓMICOS Y TRANSFORMACIÓN DIGITAL
SECRETARÍA DE ESTADO DE TELECOMUNICACIONES E INFRAESTRUCTURAS DIGITALES
Plan de Recuperación, Transformación y Resiliencia
UNICO I+D

It can be said that there would be one for each blimp, we will call them i (left) and d (right). We would have:

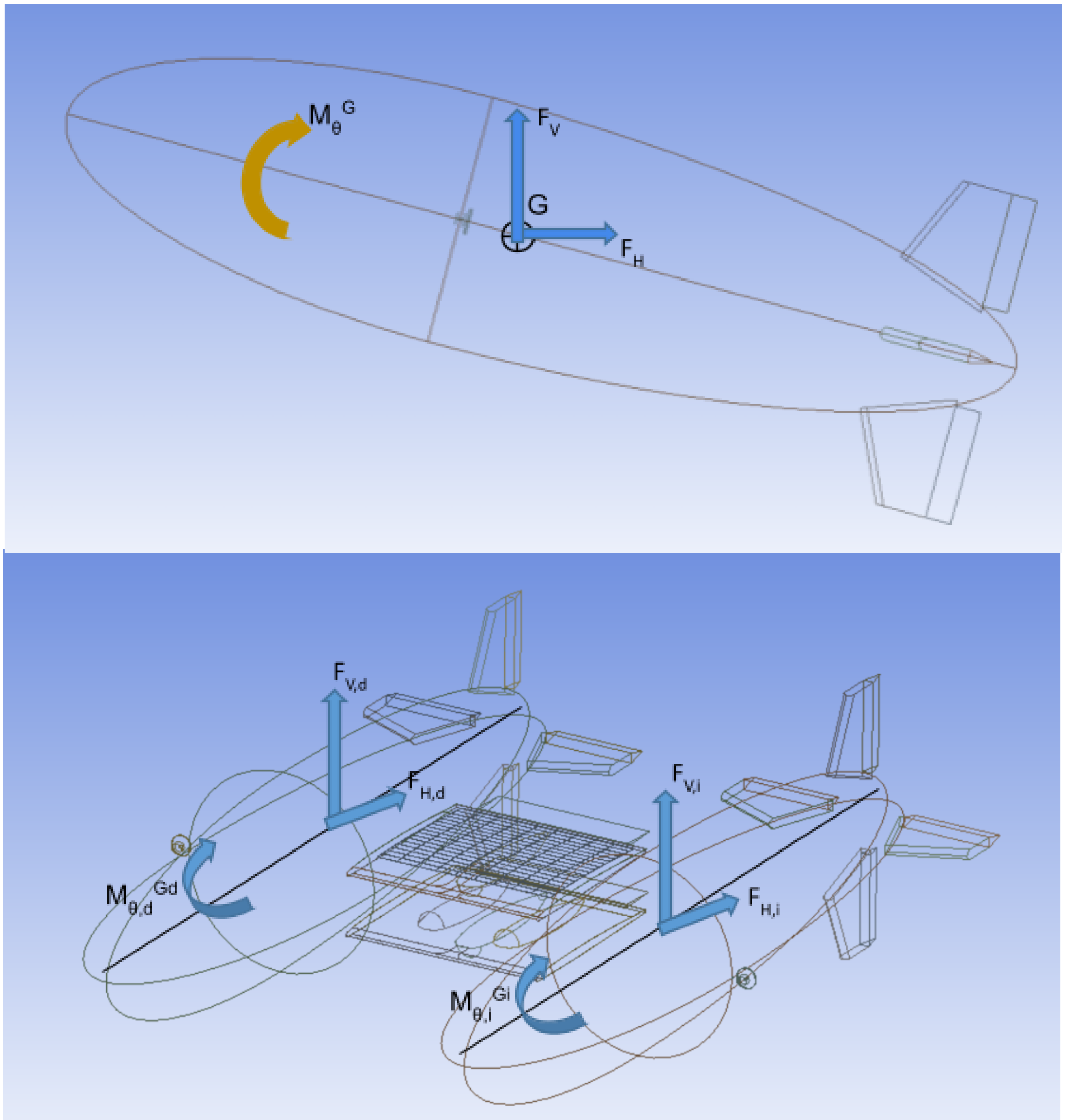

FIGURE 3.2-1 FORCES AND MOMENT SYSTEM IN BOTH BLIMPS

3.3. Wings. Definitions

The longitudinal equations of stability and control for the double wing will be developed with the parameters and variables shown in the following image. Reference frames can also be seen.

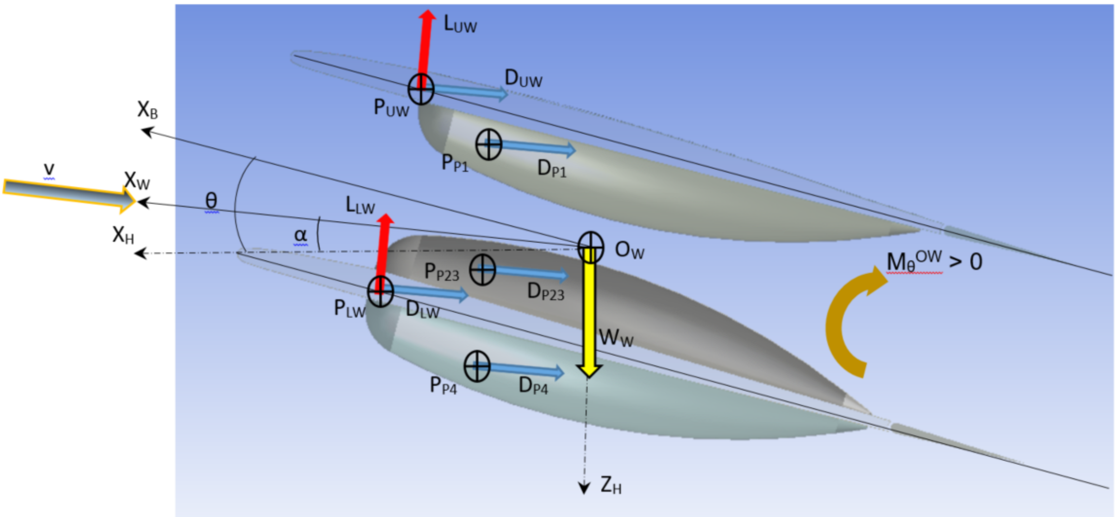

FIGURE 3.3-1 LONGITUDINAL PARAMETERS AND VARIABLES OF THE DOUBLE WING

Every parameter and variable used are described below:
$W_W=W_{P1}+W_{P2}+W_{P3}+W_{P4}+W_{UW}+W_{LW}$ · Weight of pods (1 to 4) upper and lower wings

O_W · Center of gravity of the group (point with respect to which the sum of the moments of the weights is zero)

D_{P1}, D_{P2}, $D_{P23} = D_{P2}+D_{P3}$ Aerodynamic drag of each pod (1 to 4)

$L_{UW} = \frac{1}{2}\rho_a v^2 S_W C_{L_W}(\alpha)$ Aerodynamic lift Upper Wing

$L_{LW} = \frac{1}{2}\rho_a v'^2 S_W C_{L_W}(\alpha)$ Aerodynamic lift Lower Wing

$C_{L_W}(\alpha)$ · Aerodynamic lift coefficient of wing profiles

S_W · Wings "wet" surfaces

$D_{UW} = \frac{1}{2}\rho_a v^2 S_W C_{D_W}\left(C_{L_W}, \alpha\right)$ Aerodynamic drag Upper Wing

$D_{LW} = \frac{1}{2}\rho_a v'^2 S_W C_{D_W}\left(C_{L_W}, \alpha\right)$ Aerodynamic drag Lower Wing

$C_{D_W}\left(C_{L_W}, \alpha\right)$ · Aerodynamic drag coefficient of wing profile

v · Velocity "seen" by the upper wing

v' · Velocity "seen" by the lower wing

P_{UW} · Center of pressure of upper wing (x_{BPUW},y_{BPUW},z_{BPUW}) · Coordinates in body frame

Financiado por la Unión Europea NextGenerationEU
GOBIERNO DE ESPAÑA
MINISTERIO DE ASUNTOS ECONÓMICOS Y TRANSFORMACIÓN DIGITAL
SECRETARÍA DE ESTADO DE TELECOMUNICACIONES E INFRAESTRUCTURAS DIGITALES
Plan de Recuperación, Transformación y Resiliencia
UNICO I+D

P_{LW} · Center of pressure of lower wing (x_{BPLW},y_{BPLW},z_{BPLW}) · Coordinates in body frame

P_{P1} · Center of pressure of pod 1 (x_{BPP1},y_{BPP1},z_{BPP1}) · Coordinates in body frame

P_{P23} · Center of pressure of pods 2 and 3 (x_{BPP23},y_{BPP23},z_{BPP23}) · Coordinates in body frame

P_{P4} · Center of pressure of pod 4 (x_{BPP4},y_{BPP4},z_{BPP4}) · Coordinates in body frame

Notes:

All the reference frames have its origins in Ow.

The equation of moments is calculated with respect to Ow.

Assumed that the velocities that "see" the upper and lower wing could be different to each other and in general different to the velocity of the airship itself due to the interference between both wings and of the wings with the blimps. In further improvements should be evaluated via CFD (Computational Fluids Dynamics).

3.4. Wings. Equations

The equations are:

VERTICAL FORCES

$$F_{V,W} = W_W - \left(L_{UW} + L_{LW}\right)cos(\alpha) + \left(D_{UW} + D_{LW} + D_{P1} + D_{P23} + D_{P4}\right)sin(\alpha)$$

Equation 3.4-1 **Double wing vertical forces**

HORIZONTAL FORCES

$$F_{H,W} =- \left(L_{UW} + L_{LW}\right)sin(\alpha) - \left(D_{UW} + D_{LW} + D_{P1} + D_{P23} + D_{P4}\right)cos(\alpha)$$

Equation 3.4-2 **Double wing horizontal forces**

MOMENTS RESPECT TO Ow

$$M_{\theta,W}^{OW} = (D_{UW}z_{BPUW} + D_{LW}z_{BPLW} + D_{P1}z_{BPP1} + D_{P23}z_{BPP23} + D_{P4}z_{BPP4} + L_{UW}x_{BPUW} + L_{LW}x_{BPLW})\cos(\theta - \alpha) + (D_{UW}x_{BPUW} + D_{LW}x_{BPLW} + D_{P1}x_{BPP1} + D_{P23}x_{BPP23} + D_{P4}x_{BPP4} + L_{UW}z_{BPUW} + L_{LW}z_{BPLW})sin(\theta - \alpha)$$

Equation 3.4-3 **Double wing longitudinal moments**

These equations are included to complete the development and would be useful to find the optimal location of the masses of the pods and other geometrical values, but could be assumed that the

Financiado por la Unión Europea NextGenerationEU
GOBIERNO DE ESPAÑA MINISTERIO DE ASUNTOS ECONÓMICOS Y TRANSFORMACIÓN DIGITAL SECRETARÍA DE ESTADO DE TELECOMUNICACIONES E INFRAESTRUCTURAS DIGITALES
Plan de Recuperación, Transformación y Resiliencia
UNICO I+D

contribution of the forces and moments to the global value should be negligible with respect to the blimps contribution due to the difference in mass and inertia, also should be the stability contribution. Anyway, it should be checked that the difference between forces due to wings and to blimps does not produce high structural loads in the interface between them.

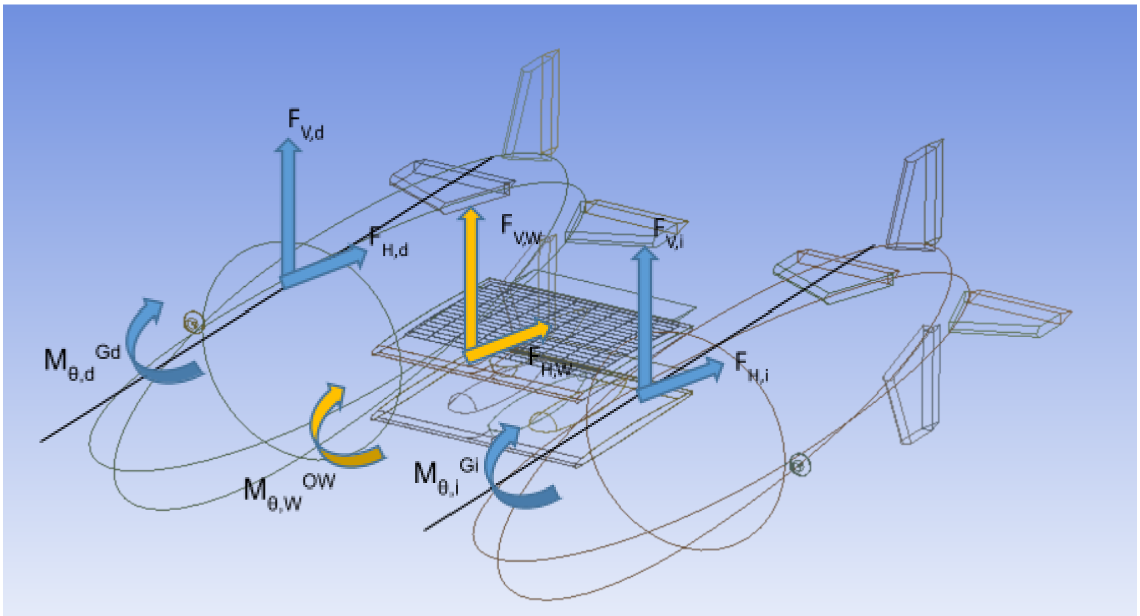

FIGURE 3.4-1 LONGITUDINAL FORCES AND MOMENTS SYSTEM

4. Implementation and use of equations

4.1. Characterization of variables. Wings and tail fins aerodynamic

The next step would be to characterize all the individual terms in the equations, specially the aerodynamic ones.

All the aerodynamic variables relative to wings and fins which are formed by standard NACA aerodynamic profiles are characterized as usual with the well-known equations:

$$L = \frac{1}{2}\rho v^2 S C_l(\alpha) \; D = \frac{1}{2}\rho v^2 S C_D(\alpha)$$

So, except for some variations in the velocity for each specific case, the problem is reduced to obtain the values of C_L and C_D which depends on the profile chosen is each case. In this phase of the project the NACA 0021 profile have been chosen.

It is a symmetric profile, chosen because the lift would be zero when the angle of attack is zero which is taken as a design decision. When the angle of attack of the airship is zero, not additional lift is required,

Financiado por la Unión Europea NextGenerationEU
GOBIERNO DE ESPAÑA MINISTERIO DE ASUNTOS ECONÓMICOS Y TRANSFORMACIÓN DIGITAL SECRETARÍA DE ESTADO DE TELECOMUNICACIONES E INFRAESTRUCTURAS DIGITALES
Plan de Recuperación, Transformación y Resiliencia
UNICO I+D

actually the buoyancy should be enough to keep the airship in-flight. Additional and localized lift will be required for maneuvers only. Besides that in a symmetric profile the center of pressure is precisely localized in a quarter of the chord which simplifies and reduces the number of variables,

NACA 0021 Profile (parameters curves obtained for Re = 10^6)

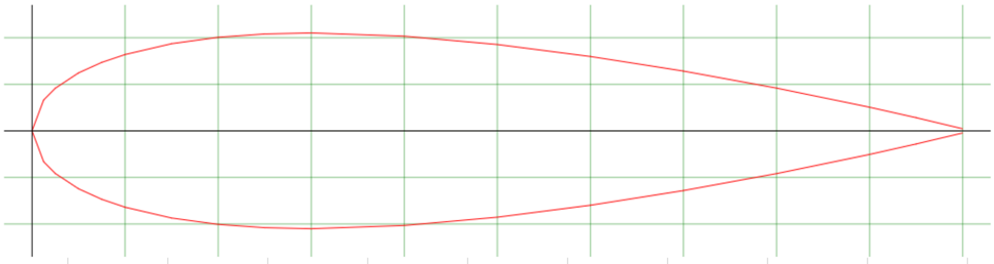

FIGURE 4.1-1 NACA 0021 PROFILE SHAPE

Financiado por la Unión Europea NextGenerationEU
GOBIERNO DE ESPAÑA MINISTERIO DE ASUNTOS ECONÓMICOS Y TRANSFORMACIÓN DIGITAL SECRETARÍA DE ESTADO DE TELECOMUNICACIONES E INFRAESTRUCTURAS DIGITALES
Plan de Recuperación, Transformación y Resiliencia
UNICO I+D

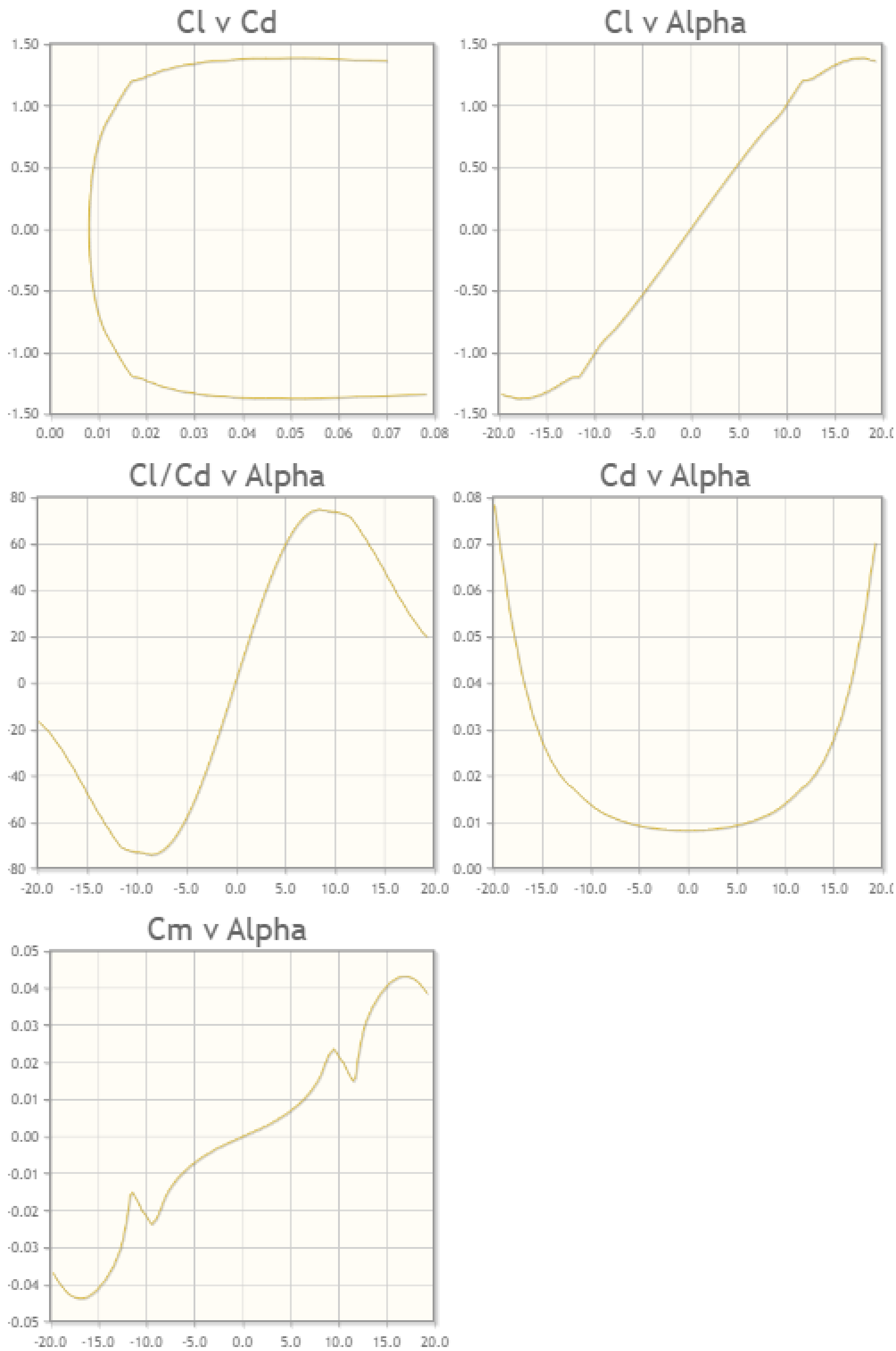

FIGURE 4.1-2 NACA 0021 PROFILE PARAMETERS VALUES VS A

Financiado por la Unión Europea NextGenerationEU
GOBIERNO DE ESPAÑA
MINISTERIO DE ASUNTOS ECONÓMICOS Y TRANSFORMACIÓN DIGITAL
SECRETARÍA DE ESTADO DE TELECOMUNICACIONES E INFRAESTRUCTURAS DIGITALES
Plan de Recuperación, Transformación y Resiliencia
UNICO I+D

This graph are converted to equations in the range of angle of attack of our interest which currently is fixed in ±10°, such as:

$$C_{Lt} = a_{Lt}\alpha$$
$$C_{Dt} = b_{4t}\alpha^4 + b_{3t}\alpha^3 + b_{2t}\alpha^2 + b_{1t}\alpha + b_{0t}$$

aLt	0,1		NACA 0021
b4t	3,00E-07		NACA 0021
b3t	-2,00E-18		NACA 0021
b2t	7,00E-05		NACA 0021
b1t	7,00E-16		NACA 0021
b0t	0,0096		NACA 0021

TABLE 4.1-1 SUMMARY

4.2. Characterization of variables. Blimps aerodynamics

The aerodynamic characterization of the blimp beyond the buoyancy (governed by the Archimedes principle) is a very different issue.
Currently the blimps shape are considered as *NPL shape*; this was suggested by the National Physics Laboratory of England and can be considered as an intersection of two ellipses with different major axes and same minor axes. The equations of shape construction are clarified in the following image.

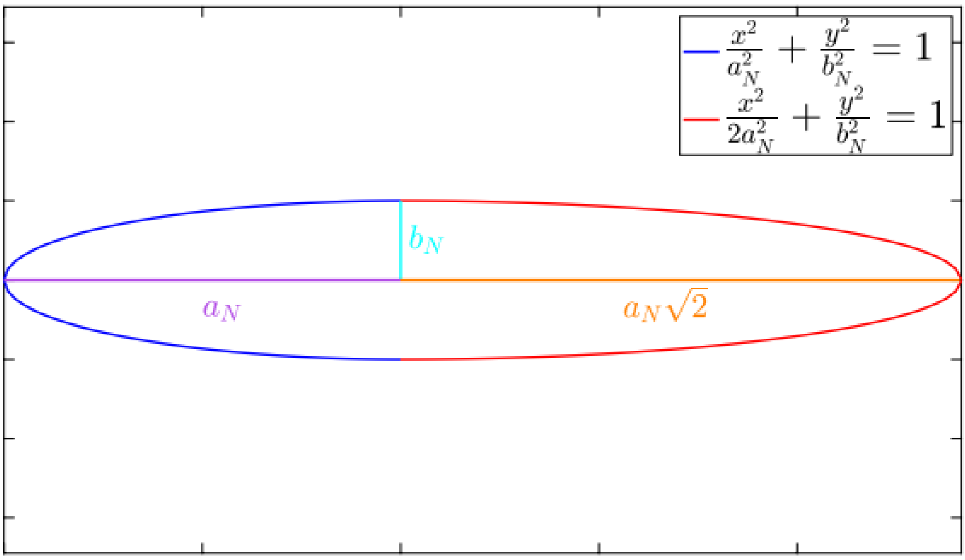

FIGURE 4.2-1 NPL SHAPE

Other shapes that could be implemented in further development would be:

GNVR shape: Developed by National Aerospace Laboratories. Consists of three parts: Semi-ellipse, sector of a circle and sector of parabola. The equations of shape construction are clarified in the following image.

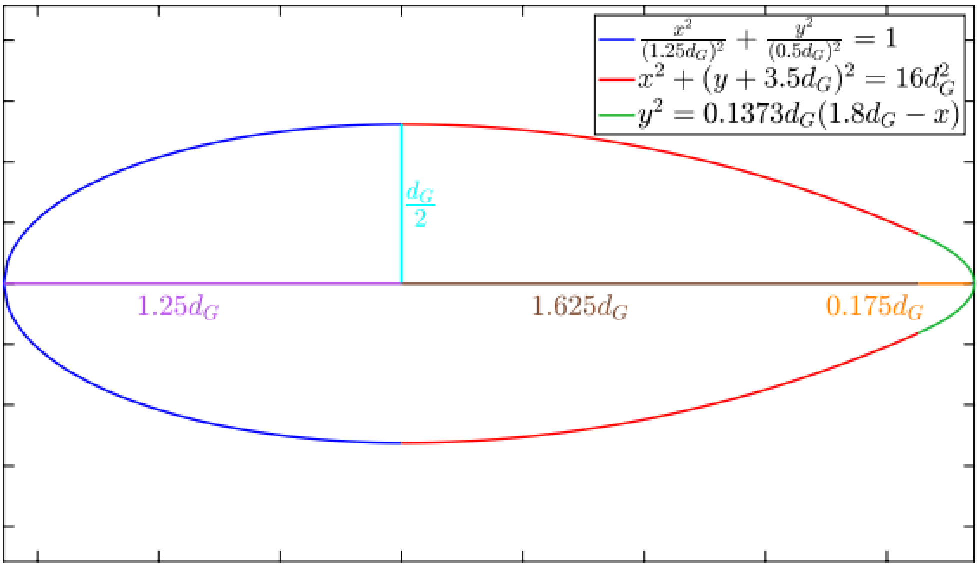

Figure 4.2-2 GNVR Shape

Wang shape: Is developed by a parametric equation clarified in the following image:

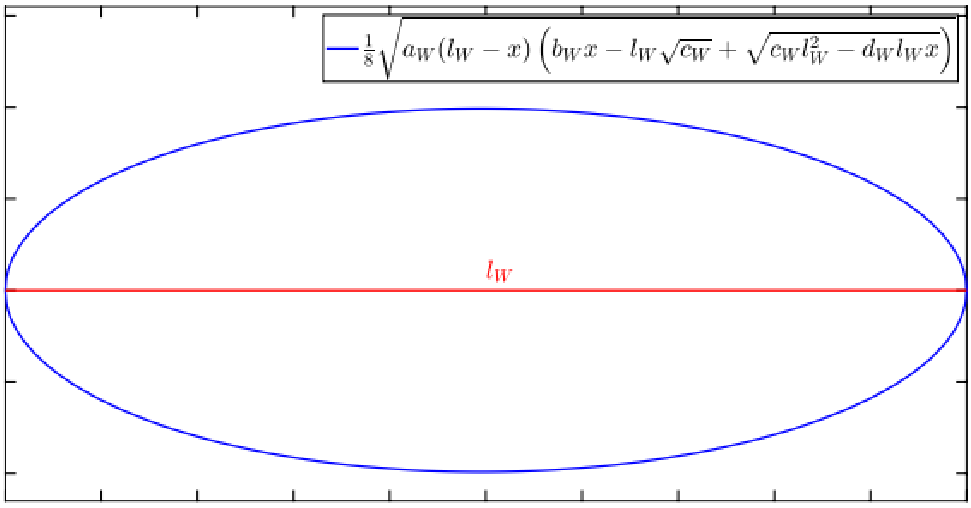

Figure 4.2-3 Wang Shape

The aerodynamic analysis of the airship hull was developed by Munk based on slender body assumption and potential flow theory, then modified by Allen and Perkins with empirical part to simulate the effect of viscosity on the normal force per unit hull length considering that each local cross section as an infinite-length circular cylinder placed normal to the flow. Also, Hopkins

Financiado por la Unión Europea NextGenerationEU
GOBIERNO DE ESPAÑA
MINISTERIO DE ASUNTOS ECONÓMICOS Y TRANSFORMACIÓN DIGITAL
SECRETARÍA DE ESTADO DE TELECOMUNICACIONES E INFRAESTRUCTURAS DIGITALES
Plan de Recuperación, Transformación y Resiliencia
UNICO I+D

developed a semi-empirical equation to compute the normal force per unit hull length. The solution over the hull body is splitted into two parts. The first one is computed by Munk's model [ref.12] whereas the second one is obtained by Hopkin's model based on body revolution at low angles of attack.

The effect of fins is added by Jones and DeLaurier considering the analysis is divided into two regimes. The first one starts from airship's nose to the position of fins leading edge and the second is the extended body shape. Although these models were developed for uniform flow, they can achieve stability for large side-slip angle of finned airships. Jones and DeLaurier model [ref.8] was verified to be the best one. The equations of this model depend on two categories of free parameters. The first category is related to the airship hull which are the minor axes (b), the average of the major axes (a) and the location of the leading edge of airship fin (lh). The second category is related to the airship fin which are fin chord (c), fin span (bf) and the maximum thickness to chord ratio of fin (t/c)max. Yuwen Li and Meyer Nahon [ref.13] use Hopkins and Finck [ref.14,15] semi-empirical model to deduce the aerodynamic governing equation in space and verify it with CFD. In this study, the kinetics of aerodynamics in space is developed by Jones and DeLaurier model.

A brief description of the Jones and DeLaurier model is presented below:

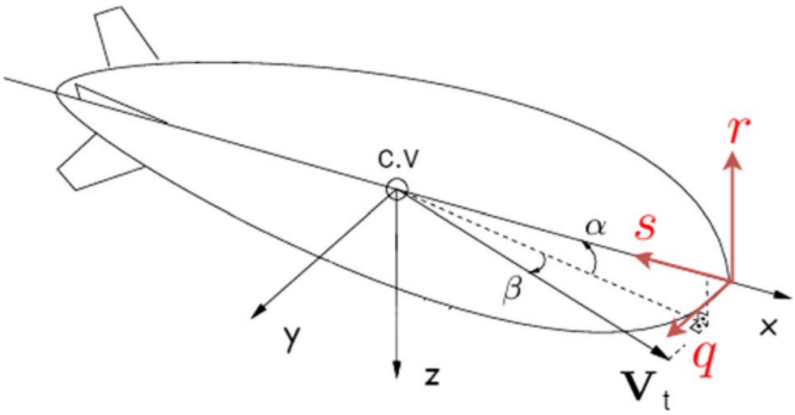

Figure 4.2-4 Airship aerodynamic axes

The aerodynamic equations developed by Jones and DeLaurier were introduced at airship nose for uniform flow, so the heading velocity projection is taken in sr-plane, to be:

$$\begin{bmatrix} F_{s,\alpha} \\ F_{r,\alpha} \\ L_{s,\alpha} \\ M_{q,\alpha} \end{bmatrix} = \frac{1}{2}\rho V_{t,\alpha}^2 \begin{bmatrix} C_{X,\alpha} \\ C_{Z,\alpha} \\ C_{L,\alpha} \\ C_{M,\alpha} \end{bmatrix}$$

Where

Financiado por la Unión Europea NextGenerationEU
GOBIERNO DE ESPAÑA
MINISTERIO DE ASUNTOS ECONÓMICOS Y TRANSFORMACIÓN DIGITAL
SECRETARÍA DE ESTADO DE TELECOMUNICACIONES E INFRAESTRUCTURAS DIGITALES
Plan de Recuperación, Transformación y Resiliencia
UNICO I+D

$$C_{X,\alpha} = C_{X1}\cos^2(\alpha) + C_{X2}\sin(2\alpha)\sin\left(\frac{\alpha}{2}\right)$$

$$\begin{aligned} C_{Z,\alpha} = & C_{Z1}\cos\left(\frac{\alpha}{2}\right)\sin(2\alpha) + C_{Z2}\sin(2\alpha) \\ & + C_{Z3}\sin(\alpha)\sin(|\alpha|) \\ & + C_{Z4}(\delta_{eL} + \delta_{eR}) \end{aligned}$$

$$C_{L,\alpha} = C_{L1}(\delta_{eR} - \delta_{eL})$$

$$\begin{aligned} C_{M,\alpha} = & C_{M1}\cos\left(\frac{\alpha}{2}\right)\sin(2\alpha) + C_{M2}\sin(2\alpha) \\ & + C_{M3}\sin(\alpha)\sin(|\alpha|) \\ & + C_{M4}(\delta_{eL} + \delta_{eR}) \end{aligned}$$

The aerodynamic constants C_{X1}, C_{X2}, C_{Z1}, C_{Z2}, C_{Z3}, C_{Z4}, C_{M1}, C_{M2}, C_{M3} and C_{M4} are given by

$$C_{X1} = C_{Dh0}S_h + C_{Df0}S_f$$

$$C_{X2} = -(k_2 - k_1)\eta_k I_1$$

$$C_{Z1} = -C_{X2}$$

$$C_{Z2} = \frac{1}{2}\left(\frac{\partial C_l}{\partial \alpha}\right)_f S_f \eta_f$$

Financiado por la Unión Europea NextGenerationEU
GOBIERNO DE ESPAÑA
MINISTERIO DE ASUNTOS ECONÓMICOS Y TRANSFORMACIÓN DIGITAL
SECRETARÍA DE ESTADO DE TELECOMUNICACIONES E INFRAESTRUCTURAS DIGITALES
Plan de Recuperación, Transformación y Resiliencia
UNICO I+D

$$
\begin{aligned}
C_{Z3} &= C_{Dch}J_1 + C_{Dcf}S_f \\
C_{Z4} &= \left(\frac{\partial C_l}{\partial \delta}\right)_f S_f \eta_f \\
C_{L1} &= \left(\frac{\partial C_l}{\partial \delta}\right)_f S_f \eta_f l_{f3} \\
C_{M1} &= -(k_2 - k_1)\eta_k I_3 \\
C_{M2} &= -\frac{1}{2}\left(\frac{\partial C_l}{\partial \alpha}\right)_f S_f \eta_f l_{f1} \\
C_{M3} &= -\left(C_{Dch}J_2 + C_{Dcf}S_f l_{f2}\right) \\
C_{M4} &= -\left(\frac{\partial C_l}{\partial \delta}\right)_f S_f \eta_f l_{f1}
\end{aligned}
$$

The aerodynamic constants and geometric variables are given by

$$
\begin{aligned}
S_{fh} = a_2 b \Bigg[& \frac{(x_2 - a_1)\sqrt{a_2^2 - (x_2 - a_1)^2}}{a_2^2} \\
& - \frac{(x_1 - a_1)\sqrt{a_2^2 - (x_1 - a_1)^2}}{a_2^2} \\
& + \sin^{-1}\left(\frac{x_2 - a_1}{a_2}\right) - \sin^{-1}\left(\frac{x_1 - a_1}{a_2}\right) \Bigg]
\end{aligned}
$$

$$
\begin{aligned}
I_1 &= \int_0^{l_h} \frac{\mathrm{d}A(s)}{\mathrm{d}s}\mathrm{d}s \\
&= \pi b^2 \left[1 - \left(\frac{l_h - a_1}{a_2}\right)^2\right]
\end{aligned}
$$

Financiado por la Unión Europea NextGenerationEU
GOBIERNO DE ESPAÑA MINISTERIO DE ASUNTOS ECONÓMICOS Y TRANSFORMACIÓN DIGITAL SECRETARÍA DE ESTADO DE TELECOMUNICACIONES E INFRAESTRUCTURAS DIGITALES
Plan de Recuperación, Transformación y Resiliencia
UNICO I+D

$$
\begin{aligned}
I_3 &= \int_0^{l_h} s\frac{\mathrm{d}A(s)}{\mathrm{d}s}\mathrm{d}s \\
&= \frac{\pi b^2}{3}\left[a_1 - \frac{1}{a_2^2}\left(2l_h^3 - 3a_1 l_h^2 + a_1^3\right)\right]
\end{aligned}
$$

$$
\begin{aligned}
J_1 &= \int_0^{l_h} 2r(s)\mathrm{d}s \\
&= \frac{1}{2}a_1 b\pi + a_2 b\left[\frac{(l_h - a_1)\sqrt{a_2^2 - (l_h - a_1)^2}}{a_2^2}\right. \\
&\quad \left. + \sin^{-1}\left(\frac{l_h - a_1}{a_2}\right)\right]
\end{aligned}
$$

$$
\begin{aligned}
J_2 &= \int_0^{l_h} 2r(s)s\mathrm{d}s \\
&= 2a_1^2 b\left(\frac{\pi}{4} - \frac{1}{3}\right) \\
&\quad + 2a_2 b\left[\frac{a_2}{3}\left(1 - \left(1 - \left(\frac{l_h - a_1}{a_2}\right)^2\right)^{3/2}\right)\right. \\
&\quad - \frac{a_1}{2}\left(\left(\frac{l_h - a_1}{a_2}\right)\sqrt{1 - \left(\frac{l_h - a_1}{a_2}\right)^2}\right. \\
&\quad \left.\left. + \sin^{-1}\left(\frac{l_h - a_1}{a_2}\right)\right)\right]
\end{aligned}
$$

The drag coefficients C_{Dh0} and C_{Df0} can be obtained from Hoerner [ref.10] and Sadraey [ref.11] , respectively

Financiado por la Unión Europea NextGenerationEU
GOBIERNO DE ESPAÑA MINISTERIO DE ASUNTOS ECONÓMICOS Y TRANSFORMACIÓN DIGITAL SECRETARÍA DE ESTADO DE TELECOMUNICACIONES E INFRAESTRUCTURAS DIGITALES
Plan de Recuperación, Transformación y Resiliencia
UNICO I+D

$$C_{Dh0} = \frac{1}{Re_{l_h}^{1/6}}\left[0.172\left(\frac{l_h}{2b}\right)^{1/3} + 0.252\left(\frac{l_h}{2b}\right)^{-1.2} + 1.032\left(\frac{l_h}{2b}\right)^{-2.7}\right]$$

$$C_{Df0} = C_f\left(\frac{S_{wet}}{S_f}\right)\left(\frac{Cd_{\min}}{0.004}\right)^{0.4}\left(1 - 0.08M_{no}^{1.45}\right)\left[1 + 2.7\left(\frac{t}{c}\right)_{\max} + 100\left(\frac{t}{c}\right)_{\max}^{4}\right]$$

$$C_f = \begin{cases} \dfrac{1.327}{\sqrt{Re_f}} & \text{, Laminar flow} \\ \dfrac{0.455}{\left[\log_{10} Re_f\right]^{2.58}} & \text{, Turbulent flow} \end{cases}$$

$$S_{wet} = 2\left[1 + 0.5\left(\frac{t}{c}\right)_{\max}\right]S_f$$

$$S_f = b_f c \quad \text{(For Rectangular fin)}$$

The cross-flow drag coefficient, C_{Dch}, obtained by Robinson [ref.6] and C_{Dcf} computed by a regression formula developed by Wardlaw [ref.7], are as follows,

$$C_{Dch} = \begin{cases} 1 & \text{, Laminar flow} \\ 0.5 & \text{, Turbulent flow} \end{cases}$$

$$C_{Dcf} = \begin{cases} -0.1395\ AR^3 + 1.088\ AR^2 & \\ -3.418\ AR + 6.098; & \Lambda = 1 \\ -1.627\ AR^{0.5399} + 4.141; & \Lambda = 0.5 \\ -0.03513\ AR^3 + 0.2653\ AR^2 & \\ -0.9103\ AR + 2.035; & \Lambda = 0 \end{cases}$$

The fin-efficiency factor ηf and hull-efficiency factor ηk were computed by a regression formula developed by Jones and DeLaurier [ref.8], and the axial and lateral apparent-mass coefficients k1, k2 were computed by a regression formula developed by Munk [ref.9].

Financiado por la Unión Europea NextGenerationEU
GOBIERNO DE ESPAÑA MINISTERIO DE ASUNTOS ECONÓMICOS Y TRANSFORMACIÓN DIGITAL SECRETARÍA DE ESTADO DE TELECOMUNICACIONES E INFRAESTRUCTURAS DIGITALES
Plan de Recuperación, Transformación y Resiliencia
UNICO I+D

$$\begin{aligned}\eta_f =&5.649\left(\frac{S_{fh}}{S_f}\right)^7 - 17.28\left(\frac{S_{fh}}{S_f}\right)^6 \\ &+ 18.18\left(\frac{S_{fh}}{S_f}\right)^5 - 5.409\left(\frac{S_{fh}}{S_f}\right)^4 \\ &- 3.558\left(\frac{S_{fh}}{S_f}\right)^3 + 3.538\left(\frac{S_{fh}}{S_f}\right)^2 \\ &- 2.115\left(\frac{S_{fh}}{S_f}\right) + 1.006\end{aligned}$$

$$\begin{aligned}\eta_k =&1.638\left(\frac{S_f \cos^2(\Gamma)}{J_1}\right)^4 \\ &- 2.444\left(\frac{S_f \cos^2(\Gamma)}{J_1}\right)^3 \\ &+ 2.398\left(\frac{S_f \cos^2(\Gamma)}{J_1}\right)^2 \\ &+ 0.02692\left(\frac{S_f \cos^2(\Gamma)}{J_1}\right) \\ &+ 1.003\end{aligned}$$

$$k_1 =0.4964\left(\frac{a}{b}\right)^{-1.16} - 0.02019$$

$$\begin{aligned}k_2 =& - 0.000004864\left(\frac{a}{b}\right)^6 + 0.0002078\left(\frac{a}{b}\right)^5 \\ &- 0.003632\left(\frac{a}{b}\right)^4 + 0.03358\left(\frac{a}{b}\right)^3 \\ &- 0.1781\left(\frac{a}{b}\right)^2 + 0.5506\left(\frac{a}{b}\right) + 0.09385\end{aligned}$$

We are currently working on the implementation of this model in the general equations considering adaptation to the double blimp issue, signs criteria and simplifications derived of the particular configuration, such as the fact that our design has not control surfaces on the tail fins, so the terms that includes the deflection values of those (δ) are neglected.

For clarification, our design has no control surfaces because is not previewed the airship to navigate, just remains fixed in a point or a reduced area. The control required to maintain the ship in position is expected to be solved with the vectorial thrusters.

With all of these data, the problem formulation will contain following assumptions to simplify the problem and reduce some parameters:

- The range of change of attack angle (α) is [-10º,10º]
- Neglect the effect of the fin deflection (all δ = 0º)
- Symmetric airfoil of airship's fin

Financiado por la Unión Europea NextGenerationEU
GOBIERNO DE ESPAÑA
MINISTERIO DE ASUNTOS ECONÓMICOS Y TRANSFORMACIÓN DIGITAL
SECRETARÍA DE ESTADO DE TELECOMUNICACIONES E INFRAESTRUCTURAS DIGITALES
Plan de Recuperación, Transformación y Resiliencia
UNICO I+D

- No taper ratio (Λ = 1)
- No dihedral angle (Γ = 0º)
- Low speed
- Airship's fin is NACA 0021

It is previewed the creation of CFD models to verify and complete the equations and an optimization of variables via MATLAB.

4.3. Characterization of variables. Thrust

Propeller thrust is dependent on properties of the propeller and the air around it. This can be expressed in a few different ways.

We will first look at an equation for static propeller thrust, for a propeller that is stationary in a no wind condition.

Then we look at an equation for dynamic propeller thrust.

Static propeller thrust equation

Thrust is dependent on the mass flow rate on the air and the change in air velocity:

$$F_{thrust} = \dot{m} \cdot [V_e - V_0]$$

Where:

$$\dot{m} = mass\ flow\ rate$$
$$V_e = exit\ velocity\ of\ air$$
$$V_0 = entrance\ velocity\ of\ air$$

The mass flow rate can be expressed in terms of the air density, air velocity at the propeller and the area covered by the propeller:

$$\dot{m} = \rho \cdot V_p \cdot A = \rho \cdot V_p \cdot \pi r^2$$

Therefore the equation for propeller thrust can be rewritten as:

$$F_{thrust} = \rho \cdot V_p \cdot \pi r^2 \cdot [V_e - V_0]$$

While V_e and V_0 can be measured, Vp is harder to quantify. We can solve for this by thinking about thrust as the force on the propeller disk, which is equivalent to the change in pressure across the disk times the area:

$$F_{disk} = \Delta p \cdot A$$

And:

Financiado por la Unión Europea NextGenerationEU
GOBIERNO DE ESPAÑA MINISTERIO DE ASUNTOS ECONÓMICOS Y TRANSFORMACIÓN DIGITAL SECRETARÍA DE ESTADO DE TELECOMUNICACIONES E INFRAESTRUCTURAS DIGITALES
Plan de Recuperación, Transformación y Resiliencia
UNICO I+D

$$\Delta p = 0.5 \cdot \rho \cdot [V_e^2 - V_0^2]$$

Therefore:

$$F = 0.5 \cdot \rho \cdot \pi r^2 \cdot [V_e^2 - V_0^2]$$

Where:

$\rho = air\ density$

$r = propeller\ radius$

$V_e = exit\ velocity\ of\ air$

$V_0 = entrance\ velocity\ of\ air$

So in order to calculate propeller thrust, we need the air density, the radius of the propeller, and the air velocity entering and exiting the propeller.

Dynamic propeller thrust equation

When calculating dynamic propeller thrust, the forward airspeed of the propeller/aircraft as well as the rpm and propeller dimensions must be considered:

$$Thrust = 4.392x10^{-8} \cdot RPM \frac{d^{3.5}}{\sqrt{pitch}}(4.233x10^{-4} \cdot RPM \cdot pitch - V_0)$$

Where:

d = propeller diameter (in)

V_0 = propeller forward airspeed (m/s)

This empirical model applies correctional constants to bring the result closer to measured data.

Propeller thrust calculators

Some commercial propeller companies offer static and dynamic thrust calculators, which can be used to estimate the thrust produced by a propeller.

The way the calculator work is by interpolating data based on the performance of propellers the company has tested.

To calculating static thrust, the following data have to be entered:

- Diameter
- Number of blades
- Thrust by propeller
- Air density
- Motor efficiency

The dynamic calculator requires the following:

- Motor inputs (Io, Rm, KV, Efficiency)

Financiado por la Unión Europea NextGenerationEU
GOBIERNO DE ESPAÑA MINISTERIO DE ASUNTOS ECONÓMICOS Y TRANSFORMACIÓN DIGITAL SECRETARÍA DE ESTADO DE TELECOMUNICACIONES E INFRAESTRUCTURAS DIGITALES
Plan de Recuperación, Transformación y Resiliencia
UNICO I+D

- Propeller diameter
- Propeller pitch
- Air density
- Drag
- Aircraft speed

The calculator generates graphs comparing thrust and efficiency at different RPM values. They also estimate power consumption and compare your results with those for similar propeller sizes.

The calculators come with some disclaimers:

- The propeller pitch cannot be adjusted (an optimal pitch is chosen by you)
- The RPM and power values are applicable for the propellers belonging to the developer company only
- The accuracy is reduced as the number of blades increases
- Motor data should be verified with the manufacturer

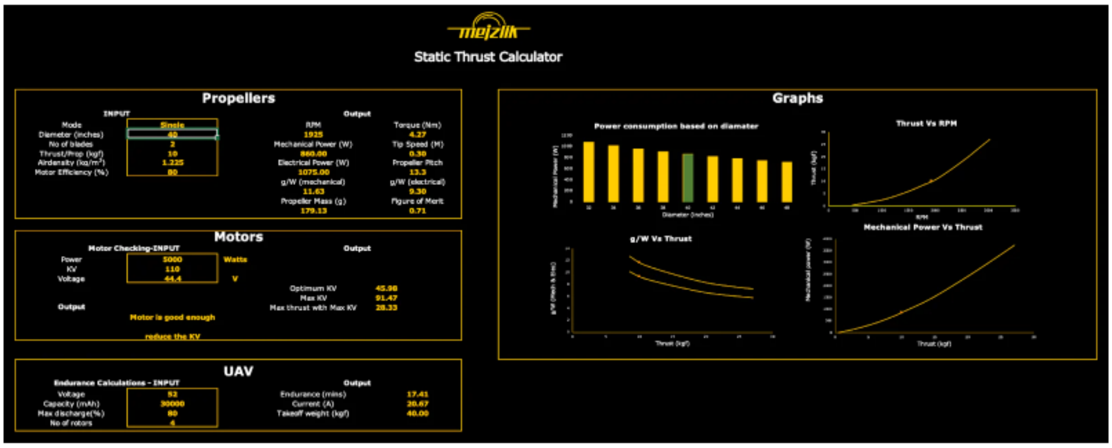

FIGURE 4.3-1 MEJZLIK'S PROPELLER STATIC THRUST CALCULATOR INTERFACE

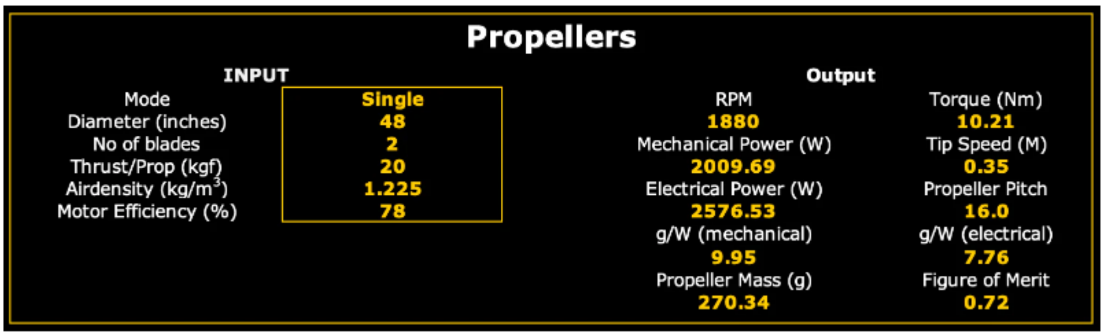

FIGURE 4.3-2 MEJZLIK'S PROPELLER THRUST CALCULATOR OUTPUT

Financiado por la Unión Europea NextGenerationEU
GOBIERNO DE ESPAÑA
MINISTERIO DE ASUNTOS ECONÓMICOS Y TRANSFORMACIÓN DIGITAL
SECRETARÍA DE ESTADO DE TELECOMUNICACIONES E INFRAESTRUCTURAS DIGITALES
Plan de Recuperación, Transformación y Resiliencia
UNICO I+D

5. Summary and Conclusions

Once the equations are completely developed, its use implies two different approximations. First, they can be used to evaluate and optimize geometric parameters such as the locations of the different forces applied, for example the total weight location (point O), the engines location (point E), the tail fins location (point Q) and the size of the tail fins can be optimized from here. The second point is to evaluate for each particular flight conditions, given by α, θ and δ angles and the flight velocity v; the values of forces and moments that appears which will allow the autopilot to compensate in case of be needed modifying engines thrust and δ or changing the distribution of masses inflating or deflating the internal ballonets to achieve optimal maneuvers performances.

The roll stability is mostly assured because of the inherent stability of airships in those axis adding the fact that the design has two symmetrical blimps which will increase stability.

On the contrary, airships are unstables in the yaw axis which should be compensated with differential thrust to avoid the circled flight. This issue will be taken into account in further iterations with a most mature geometry.

6. References

[1] *http://airfoiltools.com/airfoil/details?airfoil=naca0021-il#polars.*

[2] *https://www.mejzlik.eu/technical-data/propeller_calculator.*

[3] *J. Meseguer Ruiz, A. Sanz Andrés. Aerodinámica Básica. I.S.B.N.: 84-921113-8-0.*

[4] *M.A. Gómez Tierno, M. Pérez Cortés, C. Puentes Márquez. Mecánica del Vuelo. I.S.B.N.: 978-84-935350-2-5 Cap. 10.*

[5] *Mohamed Atyya, Gamal M. ElBayoumi and Mohamed Lotfy. Optimal shape design of an airship based on geometrical aerodynamic parameters. Beni-Suef University Journal of Basic and Applied Sciences.*

[6] Robinson M (1977) Cross-flow characteristics on a cylindrical body at incidence in subsonic fow. In: Institution of Engineers, Australian Hydraulics and Fluid Mechanics Conference, 6 th, Adelaide, Australia

[7] Wardlaw A (1979) High-angle-of-attack missile aerodynamics. Furnished to DTIC contained

[8] Jones S, DeLaurier J (1983) Aerodynamic estimation techniques for aerostats and airships. J Aircr 20(2):120–126

[9] Munk MM (1936) Aerodynamics of airships: aerodynamic theory. Springer, Berlin, pp 32–48

[10] Hoerner SF (1965) Fluid dynamic drag, published by the author. Midland Park, NJ, 16–35

[11] Sadraey M (2009) Aircraft performance: analysis. VDM Publishing, Saarbröcken

[12] Munk MM (1979) The aerodynamic forces on airship hulls. Class Aerodyn Theory 111

[13] Li Y, Nahon M (2007) Modeling and simulation of airship dynamics. J Guid Control Dyn 30(6):1691–1700

Financiado por la Unión Europea NextGenerationEU

GOBIERNO DE ESPAÑA MINISTERIO DE ASUNTOS ECONÓMICOS Y TRANSFORMACIÓN DIGITAL SECRETARÍA DE ESTADO DE TELECOMUNICACIONES E INFRAESTRUCTURAS DIGITALES

Plan de Recuperación, Transformación y Resiliencia

UNICO I+D

[14] Hopkins EJ (1951) A semi-empirical method for calculating the pitching moment of bodies of revolution at low Mach numbers

[15] Williams JE, Vukelich SR (1979) The USAF stability and control digital Datcom. Volume I. users manual. Technical report, McDonnell Douglas Astronautics Co St Louis Mo

Financiado por la Unión Europea NextGenerationEU
GOBIERNO DE ESPAÑA
MINISTERIO DE ASUNTOS ECONÓMICOS Y TRANSFORMACIÓN DIGITAL
SECRETARÍA DE ESTADO DE TELECOMUNICACIONES E INFRAESTRUCTURAS DIGITALES
Plan de Recuperación, Transformación y Resiliencia
UNICO I+D